Molecular dynamics simulation of the response of bi-disperse polyelectrolyte brushes to external electric fields*

Fen Zhang(张芬)[1], Huan-Da Ding(丁欢达)[1], Chao Duan(段超)[1], Shuang-Liang Zhao(赵双良)[2], and Chao-Hui Tong(童朝晖)[1,†]

[1] *Department of Physics, Ningbo University, Ningbo* 315211, *China*
[2] *College of Chemical Engineering, East China University of Science and Technology, Shanghai* 200237, *China*

(Received 15 March 2017; revised manuscript received 18 April 2017; published online 10 July 2017)

Langevin dynamics simulations have been performed to investigate the response of bi-disperse and strong polyacid chains grafted on an electrode to electric fields generated by opposite surface charges on the polyelectrolyte (PE)-grafted electrode and a second parallel electrode. Simulation results clearly show that, under a negative external electric field, the longer grafted PE chains are more strongly stretched than the shorter ones in terms of the relative change in their respective brush heights. Whereas under a positive external electric field, the grafted shorter chains collapse more significantly than the longer ones. It was found that, under a positive external electric field, the magnitude of the total electric force acting on one shorter PE chain is larger than that on one longer PE chain, or vice versa. The effects of smeared and discrete charge distributions of grafted PE chains on the response of PE brushes to external electric fields were also examined.

Keywords: polyelectrolyte brushes, electric fields, polydispersity, molecular dynamics

PACS: 82.35.Rs, 31.15.at, 94.20.Ss **DOI:** 10.1088/1674-1056/26/8/088204

1. Introduction

The development of "smart" nano-channels which would respond to external stimuli such as solution pH, temperature, different chemical species is one of the most important issues in the design and fabrication of highly efficient and sensitive lab-on-a-chip devices. Grafting polymer chains with ionizable functional groups onto the inner surfaces of nano-channels, thus forming a polyelectrolyte (PE) brush layer, has become probably the most effective and convenient means to fabricate "smart" nano-channels. Due to the long-range electrostatic coupling between charged polymer chains grafted on solid substrates and the released counterions, PE brushes can respond to a wider range of external stimuli such as applied electric fields than their neutral counterpart. PE brushes hold the greatest promise of smart sensing coatings for technological applications including nano-fluidic devices, drug delivery, smart valves, DNA sequencing.[1–18]

Regarding the applications of PE brushes in sensing and actuation, the swelling and collapsing of PE brushes in response to an applied electric field or voltage can be utilized to dynamically modulate electric signals in a nano-fluidic device, enabling the establishment of a gating mechanism. Due to their important applications in sensing and actuation, the response of PE brushes to external electric fields has stimulated considerable theoretical and computational research interest.[19–27] In these theoretical and computational studies, various methods such as molecular dynamics (MD) simulation and self-consistent field theory (SCFT) were employed. Using MD simulations, Ouyang *et al.* investigated the static and dynamic response of polyelectrolyte brushes with each monomer carrying a fraction of elementary charge under external electric fields.[23] Partial and full stretching of PE brushes under electric fields were observed. For electric field strength below 10^8 V/m, the brush height was found to increase with the charge fraction of monomers increasing. With grafting density increasing, due to the stronger electrostatic screening effect of charged monomers and counterions, PE brushes become less responsive to external electric fields. It was found from MD simulations that under a strongly stretching electric field, the population of grafted polyelectrolyte chains bifurcates into two subpopulations corresponding to fully and partially stretched chains, and the population weight of the fully stretched chains decreases with grafting density increasing.[24] Merlitz *et al.* examined the collapse of polyelectrolyte brushes under external electric fields by using MD simulations and developed a mean-field theory to predict the brush height.[25] Simulation results indicate that a fraction of grafted chains collapse to screen the opposite charges on the grafting electrode, while the rest of the grafted chains are not affected by the external electric fields. The MD simulations and SCFT calculations show that for PE brushes collapsing under external electric fields, the collapsed PE chains approximately compensate for the surface charges on the grafting electrode, and the counterions enriched in the immediate vicinity of the second electrode neutralize the surface charges on that electrode.[25,27] Thus, an overall charge balance near each of the two elec-

*Project supported by the National Natural Science Foundation of China (Grant No. 21374052).
†Corresponding author. E-mail: tongchaohui@nbu.edu.cn
© 2017 Chinese Physical Society and IOP Publishing Ltd

trodes is maintained. The SCFT study further revealed that for PE brushes under external electric fields, the total electric field is highly non-uniform across the two oppositely charged electrodes.[27]Comparing with strong poly(acid/base) brushes, the response of weak poly(acid/base) brushes to external electric fields has been rarely studied. Using optical ellipsometry and neutron reflectivity measurements, Weir *et al.* investigated voltage-induced swelling and deswelling of weak polybase chains grafted on an electrode.[28] At a voltage of $+1$ V or -1 V, no discernible change in the brush height was observed in experiments. We performed numerical SCFT study of the response of weak polybase brushes to surface charges on the grafting substrate immersed in a buffer solution.[29] Being consistent with experimental results, the brush height was found to be independent of the surface charge density at moderate grafting density. As a matter of fact, the local degree of ionization of weak polybase chains is affected by the applied electric field. Under an external electric field which tends to stretch the grafted chains, the local degree of ionization is suppressed which would lead to a counteracting effect on the brush height, or *vice versa*. At moderate grafting density, the two opposite effects of the external electric field on the brush height cancel each other out, resulting in the brush height independent of the external electric field.

Nonetheless, in all of these studies of the response of PE brushes to external electric fields, the charged polymer chains were assumed to be monodisperse, that is, all of the grafted polymer chains are of equal chain length. However, polydispersity is an inherent characteristic for each of all the synthetic polymers due to the great difficulty in synthesizing monodisperse polymers. Therefore, investigating the effect of polydispersity on the response of PE brushes to external electric fields is important and highly relevant to experiments.It can be expected that under external electric fields, the longer and shorter chains will not be uniformly stretched or compressed as a whole.

The present study is also motivated by an interesting experiment in which single-stranded DNAs (ssDNAs) of different chain lengths anchored onto an Au electrode through end hybridization can be separated by applying an external electric field.[16–18] The external electric field generated by applying electrode potential to the Au electrode was manipulated by gradually diluting the buffer solution contacting the Au electrode. By gradually reducing the ion concentration through dilution, thus increasing the strength of the electric field, longer ssDNA strands were detached first and then the shorter ones followed. A simple analytical model of electric double layer was proposed, which explained the experimental results semi-quantitatively. The amino-acid units in DNA are weak poly(acid/base), whose degree of ionization depends sensitively on physicochemical condition of the solution. A possible extension of the above technique is to separate strong polyelectrolytes (complete ionization in aqueous solutions) of different chain lengths by external electric fields.

It is a general practice in continuum theories such as SCFT that the discrete charges of the functional groups (completely ionized) along polymer chains are smeared along the polymer chains. It would be interesting to ask the question: how do these two different charge distributions along the grafted polymer chains affect the response of PE brushes to external electric fields?

In this paper, we present a Langevin dynamics (LD) simulational study of the response of bi-disperse PE brushes grafted on an electrode to external electric fields generated by the opposite surface charges on the grafting electrode and a second parallel electrode. The PE chains are strong polyacid, and completely ionized in an aqueous solution sandwiched between the two electrodes, and releases positively charged mono-valent counterions. Although LD simulation is much less computationally efficient than numerical SCFT calculation, it is free from the numerical instability problem incurred by SCFT calculation when grafted PE chains are stretched by external electric fields.[27] Using the probability density distributions of counterions and charged monomers obtained directly from simulations, the total electric field across the two parallel electrodes is computed through numerically solving Poisson equation. Special attention is paid to the total electric force acting on both the shorter and longer PE chains in order to validate the idea of separating strong PE chains of different chain lengths by external electric fields. In this study, the difference between smeared and discrete charge distributions along the polymer chains in terms of the response of PE brushes to external electric fields is also investigated.

2. Model and method

The bi-disperse polymer brush system was modeled as an ensemble of $M = 4 \times 4$ flexible polymer chains grafted on a square lattice with dimensions $L_x \times L_y$ (xy plane) situated at $z = 0$. Half of the polymer chains are composed of $N = 96$ monomers and the other half are composed of $N = 48$ monomers. The longer and shorter chains were uniformly grafted on the electrode at $z = 0$. A second wall at $z = L_z$ closes the system. The polymer brushes were immersed in a salt-free aqueous solution sandwiched between the two walls.Periodic boundary conditions were applied only in x and y directions.

The longer and shorter grafted chains were assumed to carry a total quantity of 8 and 4 negative elementary charges, respectively. For the smeared charged distribution denoted as S, each individual monomer in a grafted chain carries an equal fraction of charges, i.e., $1/12$. Whereas for the discrete charge distribution, starting from the first charged monomer closest to the grafting electrode, two neighboring charged monomers

are separated by 10 neutral monomers. For the discrete charge distribution, three types of grafted chains denoted as $D1$, $D2$, and $D3$, which differed in the position of the first charged monomer, were considered in this study and are illustrated in Fig. 1.

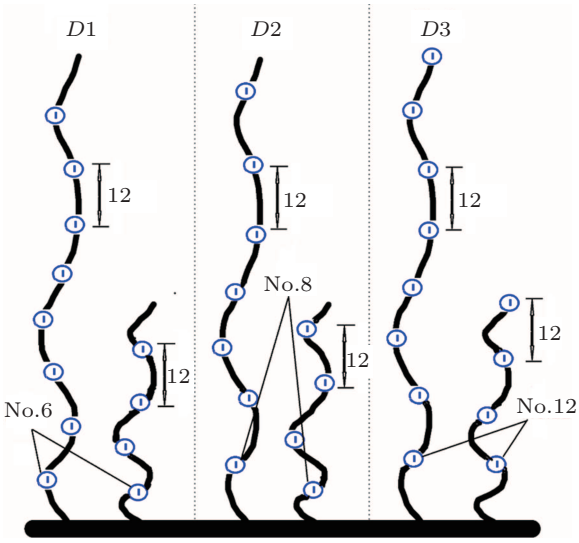


Fig. 1. (color online) Schematic representation of the three types of grafted chains denoted as $D1$, $D2$, and $D3$. The first charged monomers correspond to the 6th, 8th, and 12th monomers counting from the first monomer anchored on the grafting electrode for $D1$, $D2$, and $D3$, respectively.

The external electric field $\boldsymbol{E}$ was applied along the z direction perpendicular to the two parallel walls. The motion of particle i with mass m_i at position $\boldsymbol{r}_i(t)$ is described by Langevin equation:

$$m_i \frac{\mathrm{d}^2 \boldsymbol{r}_i}{\mathrm{d}t^2} = -\zeta_i \frac{\mathrm{d}\boldsymbol{r}_i}{\mathrm{d}t} - \nabla_i U_{\text{total}} + q_i e \boldsymbol{E} + \boldsymbol{\eta}_i, \tag{1}$$

where ζ_i is the friction coefficient which couples the particle to a heat bath; $\boldsymbol{\eta}_i$ represents the random force acting on the particle and obeys the fluctuation-dissipation theorem; U_{total} is the "conservative" potential energy consisting of Lennard-Jones potential U_{LJ}, bonding potential between adjacent monomers U_{FENE}, wall potential U_{wall}, and long-range Coulomb potential U_{Coul}. All particles including neutral monomers, the charged monomers and counterions interact with each other through the Lennard-Jones potential:

$$U_{\text{LJ}}(r_{ij}) = \begin{cases} 4\varepsilon \left[\left(\dfrac{\sigma}{r_{ij}} \right)^{12} - \left(\dfrac{\sigma}{r_{ij}} \right)^{6} + \dfrac{1}{4} \right], & r_{ij} \le \sqrt[6]{2}\sigma, \\ 0, & r_{ij} > \sqrt[6]{2}\sigma, \end{cases} \tag{2}$$

where σ represents the nominal diameter of each particle and ε is the Lennard-Jones energy unit.[30,31]

The connectivity between neighboring monomers i, j in the same polymer chain is maintained by the finitely extensible nonlinear elastic (FENE) bond potential:

$$U_{\text{FENE}}(r_{ij}) = -\frac{1}{2} k R_0^2 \ln \left(1 - \frac{r_{ij}^2}{R_0^2} \right), \tag{3}$$

where $R_0 = 1.5\sigma$ and the spring constant $k = 30.0\varepsilon/\sigma^2$.[30,31] Such a choice of parameters for U_{FENE} gives an average bond length of 0.97σ.

Both walls are modeled as 12/6 Lennard-Jones potential:

$$U_{\text{wall}}(z) = \begin{cases} 4\varepsilon \left[\left(\dfrac{\sigma}{z} \right)^{12} - \left(\dfrac{\sigma}{z} \right)^{6} + \dfrac{1}{4} \right], & z \le \sqrt[6]{2}\sigma, \\ 0, & z > \sqrt[6]{2}\sigma, \end{cases} \tag{4}$$

where z is the distance between a particle and each of the two walls.[31]

The long-range Coulomb potential between any two charged particles is

$$U_{\text{Coul}}(r_{ij}) = k_{\text{B}} T \frac{\lambda_{\text{B}} q_i q_j}{r_{ij}}, \tag{5}$$

where $k_{\text{B}}T$ represents the thermal energy and λ_{B} denotes the Bjerrum length $\lambda_{\text{B}} = e^2/(4\pi\varepsilon_0\varepsilon_r k_{\text{B}} T)$ (ε_0 and ε_r are the vacuum permittivity and the dielectric constant of the medium, respectively). The long-range Coulomb interaction is calculated using the standard Ewald Sum technique. Because the periodic condition is broken in z the direction for the present polymer brush system, the Ewald sum was calculated in an extended system which periodically repeats the original slab system in the z direction with the insertion of an empty space between them. The empty space has twice the volume of the original slab system in this study. Furthermore, a correction term of $2\pi M_z^2/(3L_xL_yL_z)$ has been added to the Coulomb potential to cancel the inter-slab interaction due to the z component of the net dipole moment $\boldsymbol{M}$ of the repeating slabs.[23,24,31]

All particles possess the same mass m and diameter σ. The temperature of the system is $k_{\text{B}}T = 1.2\varepsilon$,[31] and the friction coefficient $\zeta_i = 1.0m\tau^{-1}$ with the time unit $\tau = \sigma(m/\varepsilon)^{1/2}$.[24] For aqueous solutions at room temperature, $\lambda_{\text{B}} = 0.71$ nm. In this study, we set $\lambda_{\text{B}} = 3\sigma$.[24] Thus, $\sigma \approx 0.24$ nm. The LD unit of the external electric field is $\varepsilon/(e\sigma) = k_{\text{B}}T/(1.2e\sigma) \cong 9.0 \times 10^7$ V/m. In this work, the electric field strength was explored up to $|\boldsymbol{E}| = 1.0$. The grafting density of polymer brushes was defined as $\sigma_{\text{g}} = M/(L_xL_y)$, which corresponds to a dimensionless grafting density $\sigma_{\text{g}}^* = \sigma_{\text{g}}\sigma^2 = M\sigma^2/(L_xL_y)$. In this work, two grafting densities, i.e., $\sigma_{\text{g}}^* = 0.0137, 0.05$, were examined.

The positions and velocities of all particles were updated by the Verlet algorithm with an integration time step of $\delta t = 0.005\tau$. It took about 4.0×10^6 time steps to bring the initial system in the absence of external electric fields into an equilibrium state. After applying external electric fields, it took another 6.0×10^6 time steps to bring the system into an equilibrium state again. Afterwards, a production-run phase with the total of 1.0×10^7 time steps follows. The data were computed by averaging over the last 1.0×10^7 time steps.

Using the charge density distributions obtained directly from simulations, the total electric field normal to the grafting

substrate was calculated through numerically solving Poisson equation. The one-dimensional (1D) Poisson equation in dimensionless form is

$$\begin{aligned}\frac{\mathrm{d}^2\psi'}{\mathrm{d}z'^2} &= -4\pi\frac{\lambda_\mathrm{B}}{\sigma}\{[|Q_\mathrm{l}|(\sigma_\mathrm{g}^{\mathrm{long}}\sigma^2)\\ &+ |Q_\mathrm{s}|(\sigma_\mathrm{g}^{\mathrm{short}}\sigma^2)]\varphi_{\mathrm{ion}}(z')\\ &- |Q_\mathrm{l}|(\sigma_\mathrm{g}^{\mathrm{long}}\sigma^2)\varphi_{\mathrm{c-m}}^{\mathrm{long}}(z')\\ &- |Q_\mathrm{s}|(\sigma_\mathrm{g}^{\mathrm{short}}\sigma^2)\phi_{\mathrm{c-m}}^{\mathrm{short}}(z').\}, \end{aligned} \tag{6}$$

where $\psi' = e\psi/(k_\mathrm{B}T)$, $z' = z/\sigma$, $|Q_\mathrm{l}|$ and $|Q_\mathrm{s}|$ denote the total charge quantities of the longer chain and shorter chains, respectively ($|Q_\mathrm{l}| = 8$, $|Q_\mathrm{s}| = 4$); $\sigma_\mathrm{g}^{\mathrm{long}}$ and $\sigma_\mathrm{g}^{\mathrm{short}}$ are the grafting densities of the longer chains and shorter chains, respectively, and in this paper $\sigma_\mathrm{g}^{\mathrm{long}} = \sigma_\mathrm{g}^{\mathrm{short}} = 0.5\sigma_\mathrm{g}$; $\phi_{\mathrm{c-m}}^{\mathrm{long}}(z')$, $\phi_{\mathrm{c-m}}^{\mathrm{short}}(z')$ are the charged monomer density distributions of the longer and shorter chains, respectively; $\phi_{\mathrm{ion}}(z')$ is the probability distribution of counterions. All of these three distributions are normalized such that

$$\int_0^{L_z} P(z)\,\mathrm{d}z = 1,$$

where $P(z)$ represent either $\phi_{\mathrm{c-m}}^{\mathrm{long}}(z)$ or $\phi_{\mathrm{c-m}}^{\mathrm{short}}(z)$, or $\phi_{\mathrm{ion}}(z)$. Using the electric potential obtained from Poisson equation, the total electric field normal to the electrodes $\boldsymbol{E}_{\mathrm{total}}$ can be calculated as follows:

$$\begin{aligned}\boldsymbol{E}_{\mathrm{total}}(z=\sigma z') &= -\boldsymbol{e}_z\,\mathrm{d}\psi/\mathrm{d}z\\ &= -\boldsymbol{e}_z(k_\mathrm{B}T/e\sigma)\,\mathrm{d}\psi'/\mathrm{d}z'. \end{aligned} \tag{7}$$

3. Results and discussions

3.1. Brush height

The response of charged polymer brushes to external electric fields in terms of the variation of brush height is illustrated in Figs. 2 and 3(a). The brush height H_B is defined as follows:

$$H_\mathrm{B} = 2\frac{\int_0^{L_z} z\phi\,(z)\,\mathrm{d}z}{\int_0^{L_z}\varphi\,(z)\,\mathrm{d}z}, \tag{8}$$

where $\phi\,(z)$ denotes the vertical monomer density distribution of the longer or shorter chains.

It can be clearly seen from Figs. 2 and 3(a) that the changes in brush height in response to applied electric fields at relatively low grafting density ($\sigma_\mathrm{g}^* = 0.0137$) are much more significant than those at high grafting density ($\sigma_\mathrm{g}^* = 0.05$). Furthermore, under a negative external electric field, the longer chains are more significantly stretched than the shorter chains at both low and high grafting densities. Taking the brush height in the absence of external electric fields as a reference, the relative changes of the brush height in parameter ranges are from +71% to −14% for longer chains and +14% to −25% for the shorter chains, respectively, as shown in Fig. 2. At higher grafting density, due to the stronger electrostatic screening from counterions and monomer charges, the relative change of the brush height is significantly reduced compared with the case of lower grafting density (from +13% to −1.5% for the longer chains and +5% to −7.8% for the shorter chain as shown in Fig. 3(a)). Thus, in terms of the relative change in brush height, the shorter PE chains collapse more strongly in a positive external electric field than the longer ones. It can be further seen from Figs. 2 and 3(a) that the brush height profiles of the three types of discrete charge distributions differ slightly from each other, and deviate from that of the smeared charged distribution as well. The relative degrees of deviation from the brush height corresponding to the smeared charge distribution in the parameter range of applied external electric fields are from 5% to −9% at lower grafting density and 7% to −4% at higher grafting density for the discrete charge distribution, respectively.

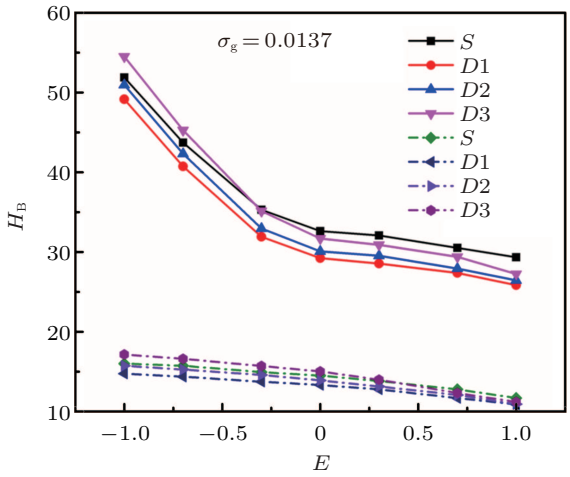


Fig. 2. (color online) Brush heights varying with the strength of external electric field at $\sigma_\mathrm{g}^* = 0.0137$. Solid and dash dotted lines correspond to longer and shorter chains, respectively.

The response of the bi-disperse PE brushes to external electric fields can also be studied by examining the ratio of mean-square end-to-end distance $\langle R_\mathrm{e}^2\rangle$ and mean-square radius of gyration $\langle R_\mathrm{g}^2\rangle$ as a function of external electric field strength, which is shown in Fig. 3(b). It is known that the ratios are 6 for ideal chains and 12 for rod-like chains in solutions, respectively.[24] Figure 3(b) clearly shows that in the absence of external electric fields, the longer chains have higher degrees of elongation than the short chains. Being consistent with the results shown in Fig. 2, at relatively low grafting density, in terms of the relative change in the ratio $\langle R_\mathrm{e}^2\rangle/\langle R_\mathrm{g}^2\rangle$, the longer chains are more significantly stretched than the shorter chains under a negative electric field. On the other hand, under a positive electric field, the ratio for the shorter chains varies

more strongly with field strength increasing than that for the longer chains.

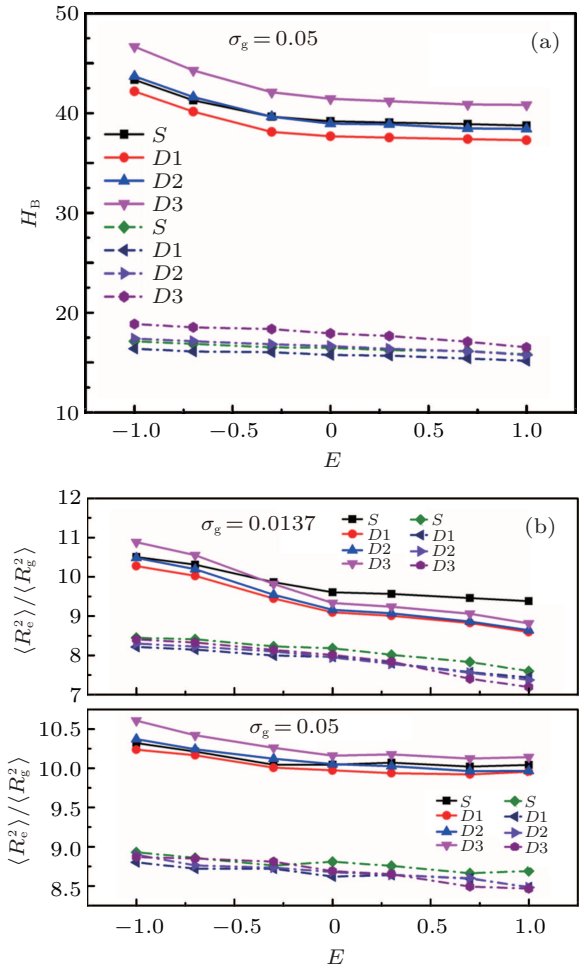


Fig. 3. (color online) (a) Brush heights varying with the strength of external electric field at $\sigma_g^* = 0.05$, and (b) conformational ratio, $\langle R_e^2\rangle/\langle R_g^2\rangle$, varying with external electric field strength at different grafting densities. The solid and dash dotted lines correspond to longer and shorter chains, respectively.

3.2. Mean electric force

The mean electric force acting on one grafted longer or shorter chain along the z direction is directly obtained from simulations as follows:

$$\boldsymbol{F}_{\text{mean}} = \sum_{i}^{N_c}[Q_i e\boldsymbol{E} - \langle \partial U_{\text{Coul}}^i/\partial z\rangle \boldsymbol{e}_z], \tag{9}$$

where Q_i is the quantity of charges on the charged monomer i ($Q_i = -1/12$ for the smeared charge distribution and $Q_i = -1$ for the discrete charge distribution), N_c is the total number of charged monomers in a grafted PE chain, U_{Coul} denotes the Coulomb potential of one charged monomer interacting with all the other charged particles in the system and the bracket refers to the ensemble average or time average, $\boldsymbol{e}_z$ is the unit vector in the z direction.

A salient feature of the mean electric force profiles shown in Figs. 4 and 5 is that the force profiles of the longer chains are on the top of those of the shorter chains. Figures 4 and 5 clearly show that under a negative external electric field which tends to stretch the grafted PE chains, the magnitude of the mean electric force acting on the longer PE chains is larger than that on the shorter chains. However, under a strong positive external electric field, the mean electric force on the shorter chains is stronger, leading to a higher degree of collapse of the shorter chains than on the longer chains. Therefore, the trends revealed from Figs. 4 and 5 are in line with the different responses of longer and shorter chains to external electric fields illustrated in Figs. 2 and 3.

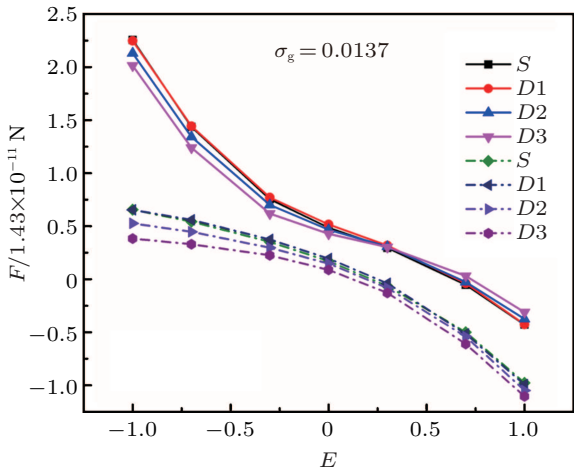


Fig. 4. (color online) Variations of mean electric force acting on each longer/shorter chain with the strength of external electric field at low grafting density $\sigma_g^* = 0.0137$. The solid and the dash dotted lines represent the longer and shorter chains, respectively.

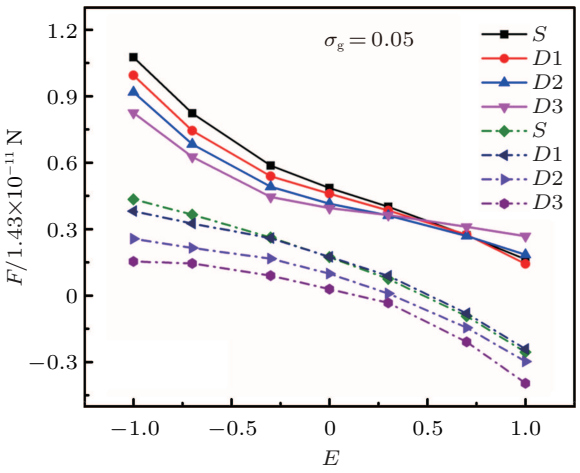


Fig. 5. (color online) Variations of mean electric force acting on each longer/shorter chain with the strength of external electric field at low grafting density $\sigma_g^* = 0.05$. The solid and the dash dotted lines represent the longer and shorter chains, respectively.

It is obvious from Figs. 4 and 5 that the magnitude of the mean electric force decreases with increasing grafting density due to the stronger electrostatic screening effect at higher grafting density. As shown in Fig. 4, at $E = -1$ corresponding to -9.0×10^7 V/m, the mean electric force acting on the longer PE chains is only about $1/4$ of the total external electric force on the longer PE chains $\sum_i^{N_c} Q_i eE = 8eE$. At higher grafting density (see Fig. 5), the mean electric force acting on

the longer PE chains at the same magnitude of external electric field is about half of that at lower grafting density. Figures 4 and 5 further show that the mean electric force profiles of the three types of discrete charge distributions slightly deviate from each other, and also differ from that of smeared charge distribution.

3.3. Total electric fields, distributions of monomers and counterions

The total electric field calculated from 1D Poisson equation is equivalent to the ensemble/time average of the instantaneous electric field at each time step in simulations, which is further averaged over the *xy* plane. As a typical example, the vertical monomer density profiles of the longer and shorter chains with the smeared charge distribution, the total electric field along the *z*axis are displayed in Figs. 6 and 7.

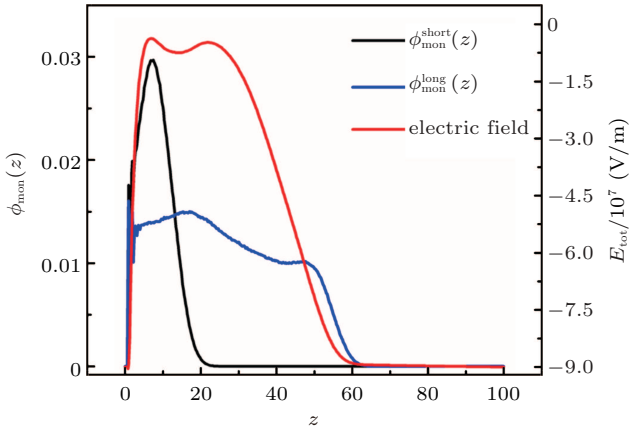


Fig. 6. (color online) Plots of total electric field and normalized monomer density distributions of the longer and shorter chains versus distance from the grafting electrode for the smeared charge distribution of grafted chains with a grafting density of $\sigma_{\rm g}^* = 0.0137$ at $E = -1.0$. Note that in this figure, the two monomer density distributions are normalized by the condition of $\int_0^{L_z} \phi^{\rm short}_{\rm mon}(z)]\,{\rm d}z + \int_0^{L_z} \phi^{\rm long}_{\rm mon}(z)\,{\rm d}z = 1$ with $\int_0^{L_z} \phi^{\rm short}_{\rm mon}(z)\,{\rm d}z = 1/3$ and $\int_0^{L_z} \phi^{\rm long}_{\rm mon}(z)\,{\rm d}z = 2/3$. In this study, equal numbers of long and short PE chains are uniformly grafted onto the electrode, and the longer chains are twice as long as the shorter ones. Thus $\int_0^{L_z} \phi^{\rm short}_{\rm mon}(z)\,{\rm d}z / \int_0^{L_z} \phi^{\rm long}_{\rm mon}(z)\,{\rm d}z = 1/2$.

As shown in Fig. 6, under a negative external electric field, the total electric field everywhere in the region between the two electrodes points to the negative z direction (negatively valued). For the smeared charge distribution, the mean electric force acting on a grafted chain can also be calculated from the following expression:

$$\boldsymbol{F}_{\rm mean} = -\boldsymbol{e}_z(k_{\rm B}T)Q\int_0^{L_z/\sigma} \phi_{\rm mon}(z')\boldsymbol{E}_{\rm total}(z')\,{\rm d}z', \quad (10)$$

where $Q = Q_{\rm l} = -8$, $Q = Q_{\rm s} = -4$ for the longer and shorter chains, respectively; $\phi_{\rm mon}$ denotes the normalized monomer density distribution of either the longer or the shorter chains ($\int_0^{L_z} \phi_{\rm mon}(z)\,{\rm d}z = 1$ for either the longer or shorter grafted chains). Note that

$$|Q_{\rm l}|\int_0^{L_z} \phi^{\rm long}_{\rm mon}(z)\,{\rm d}z = 2|Q_{\rm s}|\int_0^{L_z} \phi^{\rm short}_{\rm mon}\,{\rm d}z.$$

From the above equation and Fig. 6, it is clear that under a negative external electric field, the magnitude of mean electric force acting on one longer chain is larger than on one shorter chain.

Under a positive external electric field (see Fig. 7), the total electric field decays very quickly away from the positively charged grafting electrode. This fast decay is due to the accumulation of negative charges on the grafted PE chains near the grafting electrode which screen the external electric field.[25] As shown in Fig. 7, the total electric field drops to zero in the region around the tail of the monomer density profile of the shorter PE chains. Being further away from the grafting electrode, the total electric field changes sign and becomes negative, indicating that the negative charges on the grafted longer PE chains become the dominant factor in determining the total electric field. The negative total electric field spans the region between the tails of the monomer density profiles of the shorter and longer PE chains. In this region, the local electric force acting on the longer PE chains is positive (pointing to the positive z direction). Therefore, it is easy to understand from Eq. (10) and Fig. 7 why the magnitude of the total electric force acting on one shorter PE chain pointing to the negative z direction is larger than on one longer PE chain.

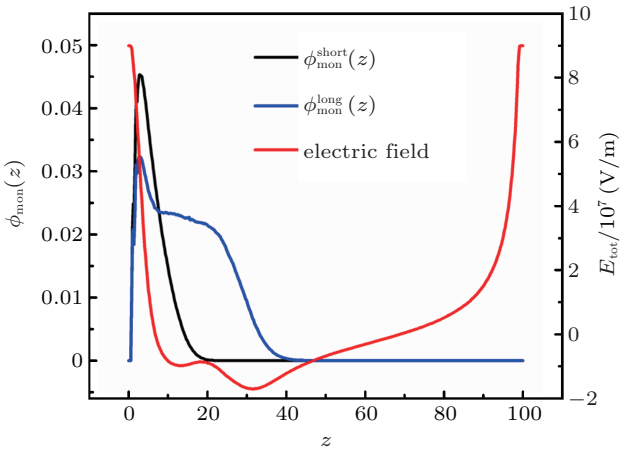


Fig. 7. (color online) Total electric field and normalized monomer density distributions of the longer and one shorter chains varying with distance from the grafting electrode for the smeared charge distribution of grafted chains with a grafting density of $\sigma_{\rm g}^* = 0.0137$ at $E = 1.0$, wher normalization condition is the same as that in Fig. 6.

MD studies of mono-disperse PE brushes reveal that the grafted chains are not uniformly stretched or compressed, but rather bifurcate into two sub-populations under external electric fields. Apparently, such a bifurcation results in the alleviation of steric and electrostatic repulsion between grafted chains. The interaction between the longer and shorter chains

is crucial to the different responses of the longer and shorter chains in the bi-disperse PE brushes to external electric fields. Under a positive external electric field, the much higher degree of collapse of the shorter chains leads to a significant reduction in the steric and electrostatic repulsion between the shorter and longer chains. On the contrary, if the longer chains were to collapse more significantly than the shorter chains, the steric and electrostatic repulsion between them would not be alleviated. Under a negative external electric field, if the shorter chains were to stretch more strongly than the longer chains, the steric and electrostatic repulsion between them would become much stronger than the case that the longer chains are more significantly stretched as revealed from simulations.

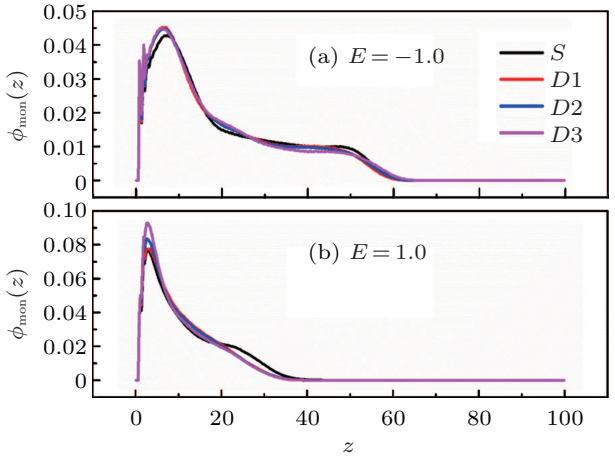


Fig. 8. (color online) Variations of total monomer density ($\phi_{\rm mon}^{\rm short}+\phi_{\rm mon}^{\rm long}$) profiles of the three types of discrete charge distributions and smeared charge distributions with distance from the grafting electrode under a strong negative (upper panel) and positive (bottom panel) at $\sigma_{\rm g}^{*}=0.0137$ are displayed.

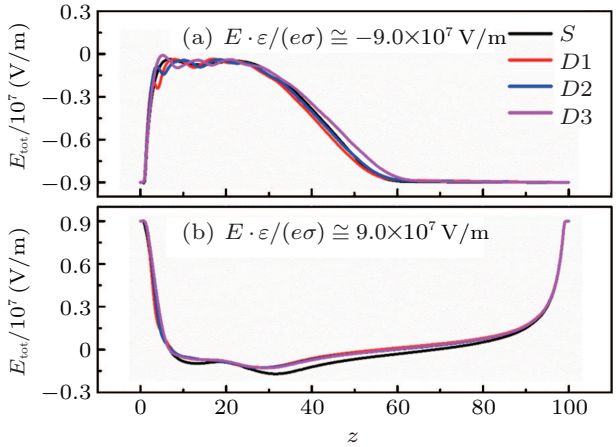


Fig. 9. (color online) Plots of the total electric fields against the distance from the grafting electrode for different charge distributions of grafted chains at different external electric field strengths: (a) $E=-1.0$, (b) $E=1.0$ (in LD unit). The grafting density corresponding to both panels (a) and (b) is $\sigma_{\rm g}^{*}=0.0137$.

It is found that under a strong negative or positive external electric field, the total monomer density profiles of the three types of discrete charge distributions only slightly deviate from that of smeared charge distribution (see Fig. 8). As shown in the upper panel of Fig. 9, under a strong negative external electric field, the total electric field corresponding to discrete charge distribution oscillates more strongly than that corresponding to smeared charge distribution near the grafting electrode. On the other hand, the total electric field profiles of the three types of discrete charge distributions almost completely overlap with each other under a strong positive external electric field.

The probability distributions of positively charged counterions along the z axis under external electric fields are examined and are shown in Fig. 10. Under a positive electric field, a fraction of counterions are expelled from the inside of PE brushes and accumulated near the negatively charged second electrode. It can be clearly seen from Fig. 10 that the fraction of counterions accumulated near the second electrode increases with increasing the strength of the positive external electric field but decreases with increasing grafting density. It is found that the total of counterions accumulated near the second electrode roughly equals that of the surface charges on the second electrode. Thus, an approximate charge balance is maintained near the second electrode. On the contrary, under a negative external electric field, counterions are strongly attracted towards the oppositely charged grafting electrode.

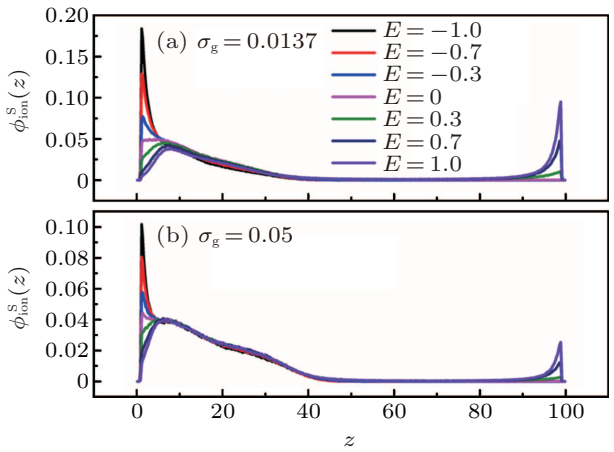


Fig. 10. (color online) Probability distributions of counterions varying with the distance from the grafting electrode in different external electric fields. The upper and bottom panels correspond to $\sigma_{\rm g}^{*}=0.0137$ and $\sigma_{\rm g}^{*}=0.05$, respectively. Note that the probability distribution of counterions is normalized such that $\int_0^{L_z}\phi_{\rm ion}^{S}(z)\,{\rm d}z=1$.

4. Conclusions

In this paper, we perform Langevin Dynamics simulations of bi-disperse PE brushes in response to external electric fields. The grafted PE chains are strong polyacid. The total electric forces acting on grafted shorter and longer PE chains are calculated. Using the charge density distributions of the brush system obtained from simulations, the total electric field across the two oppositely charged electrodes is computed by

numerically solving Poisson equations. Furthermore, the effects of smeared and discrete charge distributions of grafted PE chains on the response of PE brushes to external electric fields are also investigated.

Simulation results clearly show that, under a positive external electric field, in terms of the relative change in brush height the grafted shorter PE chains collapse more strongly than the longer PE chains in the bi-disperse brushes, and the magnitude of the total electric force acting on one shorter PE chain is larger than on one longer PE chain. On the contrary, the opposite trends are found for bi-disperse PE brushes under a negative external electric field. Under a positive external electric field, the total electric field decays quickly away from the positively charged grafting electrode. Beyond the tail region of the monomer density profile of the grafted shorter PE chains, the negative charges on the grafted longer PE chains play a dominant role in determining the total electric field, resulting in a negative total electric field in the region between the tails of the monomer density profiles of the two types of PE chains. Therefore, under a positive external electric field, the magnitude of the total electric force acting on a shorter PE chain is larger than on a longer PE chain, resulting in a higher degree of collapse of the shorter PE chains. However, under a negative external electric field, the total electric field everywhere between the two oppositely charged electrodes points towards the grafting electrode, which leads to a stronger stretching force acting on the longer PE chains. The stronger electric force stretching the grafted longer PE chains suggests that an external electric field can be used to separate strong polyelectrolyte chains based on chain length, which is similar to the scenario in the experiment of sorting ssDNA strands of different chain lengths by external electric fields.

It is found from simulations that in terms of the relative change in brush height, the discrete charge distribution deviates by no more than 10% from the smeared charge distribution. Furthermore, the profile of the total electric force acting on a grafted PE chain against the magnitude of the external electric field of the discrete charge distribution only slightly deviates from that of the smeared charge distribution. Therefore, in studying strong polyelectrolytes in mono-valent salt solutions, it is well justified to use a smeared charge distribution in continuum theories such as SCFT and ignore the discrete nature of mono-valent monomer charges.

Acknowledgement

One of the authors, Chao-Hui Tong would like to express his deep appreciation for the support from K. C. Wong Magna Fund in Ningbo University.

References

[1] Napper D H 1983 *Polymeric stabilization of colloidal dispersions* (London: Academic Press) Vol. 7
[2] Halperin A, Tirrell M and Lodge T P 1992 *Adv. Polym. Sci.* **100** 31
[3] Naji A, Seidel C and Netz R R 2006 *Adv. Polym. Sci.* **198** 149
[4] Borisov O V, Zhulina E B and Birshtein T M 1994 *Macromolecules* **27** 4795
[5] Netz R R and Andelman D 2003 *Phys. Rep.* **380** 1
[6] Naji A, Netz R R and Seidel C 2003 *Eur. Phys. J. E* **12** 223
[7] Pincus P 1991 *Macromolecules* **24** 2912
[8] Israels R, Leermaker F A M, Fleer G J and Zhulina E B 1994 *Macromolecules* **27** 3249
[9] Zhulina E B, Birshtein T M and Borisov O V 1995 *Macromolecules* **28** 1491
[10] Wynveen A and Likos C N 2009 *Phys. Rev. E* **80** 010801
[11] Russano D, Carrillo J M Y and Dobrynin A V 2001 *Langmuir.* **27** 11044
[12] Ou Y P, Sokoloff J B and Stevens M J 2012 *Phys. Rev. E* **85** 011801
[13] He S Z, Merlitz H, Chen L, Sommer J U and Wu C X 2010 *Macromolecules* **43** 7845
[14] Ibergay C, Malfreyt P and Tildesley D J 2010 *J. Phys. Chem. B* **114** 7274
[15] Guptha V S and Hsiao P Y 2014 *Polymer* **55** 2900
[16] Wu J M, Zhao S, Gao L, Wu J Z and Gao D 2011 *Lab Chip.* **11** 4036
[17] Zhao S L, Wu J M, Gao D and Wu J Z 2011 *J. Chem. Phys.* **134** 065103
[18] Wu J M, Zhao S, Gao L, Wu J Z and Gao D 2013 *J. Phys. Chem. B* **117** 2267
[19] Tsori Y, Andelman D and Joanny J F 2008 *Europhys. Lett.* **82** 46001
[20] Yamamoto T and Pincus P A 2011 *Europhys. Lett.* **95** 48003
[21] Migliorini G 2010 *Macromolecules* **43** 9168
[22] Cao Q Q, Zuo C C, Li L J and Yan G 2011 *Biomicrofluidics* **5** 044119
[23] Ouyang H, Xia Z H and Zhe J 2009 *Nanotechnology* **20** 195703
[24] Ho Y F, Shendruk T N, Slater G W and Hsiao P Y 2013 *Langmuir* **29** 2359
[25] Merlitz H, Li C, Wu C X and Sommer J U 2015 *Soft Matter* **11** 5688
[26] Meng D and Wang Q 2011 *J. Chem. Phys.* **135** 224904
[27] Tong C 2015 *J. Chem. Phys.* **143** 054903
[28] Weir M P, Heriot S Y, Martin S J, Parnell A J, Holt S A, Webster J R P and Jones R A L 2011 *Langmuir* **27** 11000
[29] Tong C 2014 *Langmuir* **30** 15301
[30] Micka U, Holm C and Kremer K 1999 *Langmuir* **15** 4033
[31] Cao Q Q, Zuo C C, He H W and Li L J 2009 *Macromol. Theory Simul.* **18** 441